The Astrophysical Journal, 726:107 (7pp), 2011 January 10 doi:10.1088/0004-637X/726/2/107

CAN GAMMA-RAY BURST JETS BREAK OUT THE FIRST STARS?

Yudai Suwa[1,2] and Kunihito Ioka[3]
[1] Department of Physics, School of Science, the University of Tokyo, 7-3-1 Hongo, Bunkyo-ku, Tokyo 113-0033, Japan
[2] Yukawa Institute for Theoretical Physics, Kyoto University, Oiwake-cho, Kitashirakawa, Sakyo-ku, Kyoto 606-8502, Japan; suwa@yukawa.kyoto-u.ac.jp
[3] KEK Theory Center and the Graduate University for Advanced Studies (Sokendai), 1-1 Oho, Tsukuba 305-0801, Japan
Received 2010 September 29; accepted 2010 November 4; published 2010 December 21

ABSTRACT

We show that a relativistic gamma-ray burst (GRB) jet can potentially pierce the envelope of a very massive first generation star (Population III, hereafter Pop III) by using the stellar density profile to estimate both the jet luminosity (via accretion) and its penetrability. The jet breakout is possible even if the Pop III star has a supergiant hydrogen envelope without mass loss, thanks to the long-lived powerful accretion of the envelope itself. While the Pop III GRB is estimated to be energetic ($E_{\gamma,\rm iso} \sim 10^{55}$ erg), the supergiant envelope hides the initial bright phase in the cocoon component, leading to a GRB with a long duration $\sim 1000(1+z)$ s and an ordinary isotropic luminosity $\sim 10^{52}$ erg s^{-1} ($\sim 10^{-9}$ erg cm^{-2} s^{-1} at redshift $z \sim 20$). The neutrino annihilation is not effective for Pop III GRBs because of a low central temperature, while the magnetic mechanism is viable. We also derive analytic estimates of the breakout conditions, which are applicable to various progenitor models. The GRB luminosity and duration are found to be very sensitive to the core and envelope mass, providing possible probes of the first luminous objects at the end of the high-redshift dark ages.

Key words: dark ages, reionization, first stars – gamma-ray burst: general – stars: general

Online-only material: color figures

1. INTRODUCTION

The ancient era of the first generation stars (Population III, hereafter Pop III)—the end of the dark age—is still an unexplored frontier in modern cosmology (Barkana & Loeb 2001; Bromm & Larson 2004; Ciardi & Ferrara 2005). The first star formation from metal-free gas has a crucial influence on subsequent cosmic evolution by producing ionizing photons and heavy elements. Although the theoretical studies were recently developed by the numerical simulations, the faint Pop III objects are difficult to observe even with future technology.

Gamma-ray bursts (GRBs) are potentially powerful probes of the Pop III era. In fact, GRB 090423 has the highest redshift $z = 8.2$ ever seen (e.g., Tanvir et al. 2009; Salvaterra et al. 2009; Chandra et al. 2010), beyond any quasars or galaxies and the previous GRB 080913 at $z = 6.7$ (Greiner et al. 2009) and GRB 050904 at $z = 6.3$ (Kawai et al. 2006; Totani et al. 2006). GRBs are presumed to manifest the gravitational collapse of a massive star—a collapsar—to a black hole (BH) with an accretion disk, launching a collimated outflow (jet) with a relativistic speed (MacFadyen & Woosley 1999). The massive stars quickly die within the Pop III era. GRBs, the most luminous objects in the universe, are detectable in principle up to redshifts $z \sim 100$ (Lamb & Reichart 2000), while their afterglows are observable up to $z \sim 30$ (Ciardi & Loeb 2000; Gou et al. 2004; Ioka & Mészáros 2005; Toma et al. 2010). As demonstrated in GRB 050904 by Subaru (Kawai et al. 2006; Totani et al. 2006), GRBs can probe the interstellar neutral fraction with the Lyα red damping wing (Miralda-Escude 1998), the metal enrichment, and the star formation rate (Totani 1997; Kistler et al. 2009). In the future, we may also investigate the reionization history (Ioka 2003; Inoue 2004), the molecular history (Inoue et al. 2007), the equation of state of the universe (Schaefer 2007; Yonetoku et al. 2004), and the extragalactic background light (Oh 2001; Inoue et al. 2010; Abdo 2010).

The first stars are predicted to be predominantly very massive $\gtrsim 100\,M_\odot$ (Abel et al. 2002; Bromm et al. 2002). The mass scale is roughly given by the Jeans mass (or the Bonnor- Ebert mass) when isothermality breaks (i.e., only through the cooling function) and hence seems robust (but see also Turk et al. 2009; Clark et al. 2010). The central part collapses first to a tiny ($\sim 0.01\,M_\odot$) protostar, followed by the rapid accretion of the surrounding matter to form a massive first star (Omukai & Palla 2003; Yoshida et al. 2008). The stars with 140–260 $M_\odot$ are expected to undergo pair-instability supernovae without leaving any compact remnant behind, while those above $\sim 260\,M_\odot$ would collapse to a massive ($\sim 100\,M_\odot$) BH with an accretion disk, potentially leading to scaled-up collapsar GRBs (Fryer et al. 2001; Heger et al. 2003; Suwa et al. 2007a, 2007b, 2009; Komissarov & Barkov 2010; Mészáros & Rees 2010). The Pop III GRB rate would be rare, ~ 0.1–10 yr^{-1}, but within reach (e.g., Bromm & Loeb 2006; Naoz & Bromberg 2007). These GRBs also mark the formation of the first BHs, which may grow to supermassive BHs via merger or accretion (Madau & Rees 2001).

However, the zero-metal stars could have little mass loss due to the line driven wind (Kudritzki 2002), and thereby have a large ($R_* \sim 10^{13}$ cm) hydrogen envelope at the end of their lives (red supergiant (RSG) phase). Especially for Pop III stars, mass accretion continues during the main-sequence phase so that the chemically homogeneous evolution induced by rapid rotation (e.g., Yoon & Langer 2005) might not work (Ohkubo et al. 2009). Their extended envelopes may suppress the emergence of relativistic jets out of their surface even if such jets were produced (Matzner 2003). The observed burst duration $T \sim 100$ s, providing an estimate for the lifetime of the central engine, suggests that the jet can only travel a distance of $\sim cT \sim 10^{12}$ cm before being slowed down to a nonrelativistic speed. This picture is also supported by the nondetections of GRBs associated with type II supernovae. Nevertheless, this may not apply to Pop III GRBs because the massive stellar accretion

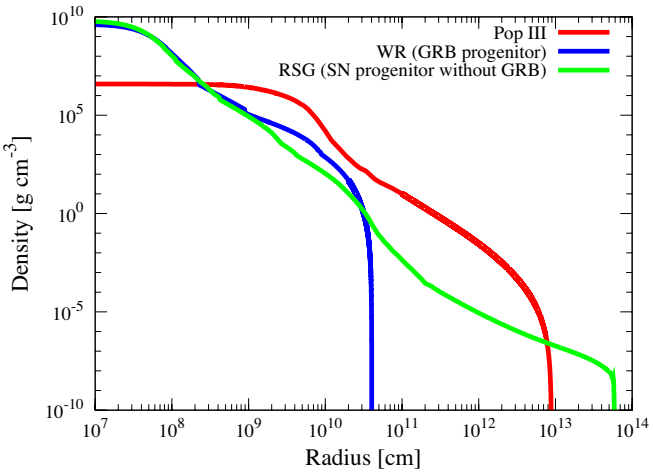

Figure 1. Density profiles of the investigated models. Red, blue, and green lines correspond to Pop III star ($M = 915\,M_\odot$), Wolf–Rayet star (W-R; GRB progenitor, $M = 16\,M_\odot$), and red supergiant (RSG; supernova progenitor without GRB, $M = 15\,M_\odot$), respectively. The Pop III and RSG have a hydrogen envelope, which expands to a large radius, while the W-R only has a core.

(A color version of this figure is available in the online journal.)

could enhance jet luminosity and duration and therefore enable the jet to break out the first stars.

In this paper, we discuss jet propagation in the first stars using the state-of-the-art Pop III stellar structure calculated by Ohkubo et al. (2009; Section 2) to estimate jet luminosity via accretion (Section 2 and 3) and to predict the main observational characteristics of Pop III GRBs, such as energy and duration. We adopt the analytical approach that reproduces the previous numerical simulations to see the dependences on the yet uncertain stellar structure (Section 6 for analytical estimates) and to avoid simulations over many digits. We determine the jet head speed that is decelerated by the shock with the stellar matter (Section 4). The shocked matter is wasted as a cocoon surrounding the jet before the jet breakout (Section 5), like in the context of active galactic nuclei (Begelman & Cioffi 1989). We treat both the jet luminosity and its penetrability with the same stellar structure consistently for the first time.

2. PROGENITOR STRUCTURE

In this paper, we employ three representative progenitors: Pop III star, Wolf–Rayet (W-R) star, and RSG. These stars correspond to progenitors of Pop III GRBs, ordinary GRBs, and core-collapse supernovae without GRBs, respectively. The W-R stars have no hydrogen envelope, which is a preferred condition for a successful jet break (Matzner 2003) and consistent with the observational evidence of GRB–SN Ibc association (Woosley & Bloom 2006).

The density profiles of investigated models are shown in Figure 1. The red line shows the density profile of the Pop III star with 915 $M_\odot$, model Y-1 of Ohkubo et al. (2009). Blue indicates the GRB progenitor with 16 $M_\odot$, model 16TI of Woosley & Heger (2006). The green line represents the progenitor of ordinary core-collapse supernovae with 15 $M_\odot$, s15.0 of Woosley et al. (2002). The density profiles are roughly divided into two parts: core and envelope. The GRB progenitor (W-R star) does not have a hydrogen envelope, while Pop III and RSG keep their envelope so that these stars experience the envelope expansion triggered by core shrinkage after the main sequence.

Because the exact stellar surface is difficult to calculate for the simulation of stellar evolution (K. Nomoto 2010, private communication), we numerically solve the equation of hydrostatic equilibrium,

$$\frac{\partial P}{\partial r} = -\frac{GM_r}{r^2}\rho, \tag{1}$$

for the outermost layer of stars, where P is the pressure, r is the radius from the center of the star, G is the gravitational constant, M_r is the mass inside r, and ρ is the density. We employ the polytropic equation of state, $P = K\rho^\gamma$, where K is the coefficient depending on the microphysics and γ is the adiabatic index. Here we use the constant value of K, fitting just outside the core. The surfaces of stars are determined by the point with $P = 0$.

We can calculate the accretion rate, $\dot{M}$, using these density profiles. The accretion timescale of matter at a radius r to fall to the center of the star is roughly equal to the free-fall timescale:

$$t_{\rm ff} \approx \sqrt{\frac{r^3}{GM_r}}. \tag{2}$$

Then we can evaluate the accretion rate at the center as $\dot{M} = dM_r/dt_{\rm ff}$. Note that our estimation neglects the effect of rotation (e.g., Kumar et al. 2008; Perna & MacFadyen 2010). However, the rotation law inside the star is very uncertain. Even though a rotationally supported disk is formed, the accretion time is roughly $\sim\alpha^{-1} = 10(\alpha/0.1)^{-1}$ times $t_{\rm ff}$, where α is the standard dimensionless viscosity parameter (Kumar et al. 2008). In addition, the jet production mechanism is also unknown and so we introduce an efficiency parameter to connect the (free-fall) mass accretion rate and jet luminosity, which will be normalized by the observed GRBs in the following section. This parameter would contain the information of both the rotation rate and the jet production efficiency.

In Figure 2, the mass accretion rates of the investigated models are shown. The origin of time in this figure is set at the time when the BH mass (central mass) is 3 $M_\odot$ (3.4 s after the onset of collapse for W-R, for instance). The accretion rate should be related to the activity of the central engine, and that of Pop III stars is much larger than the other progenitors. Therefore, the GRBs of Pop III stars are expected to be more energetic than ordinary GRBs if Pop III stars could produce GRBs. However, it is nontrivial that the GRB jets can break out the Pop III stars. In Section 4, we discuss the jet propagation and capability of a successful jet break. The colored regions in this figure show the hidden regions by the stellar interior where the jet propagates inside the star so that the high-energy photons cannot be observed.

3. JET MODELS

In this study we employ the *collapsar* model, which is a widely accepted scenario for the central engine of long GRBs. In this scenario a BH accompanied by the stellar collapse produces a relativistic jet, which is strongly suggested by observations. The greatest uncertainty in this scenario is the mechanism for converting the accretion energy or BH rotation energy into the directed relativistic outflows. There are mainly two candidates of jet production in the vicinity of the central engine: neutrino annihilation and magnetohydrodynamical (MHD) mechanisms including the Blandford–Znajek process (Blandford & Znajek 1977), which converts the BH rotation energy into the Poynting flux jet via magnetic fields. Although there are plenty of studies

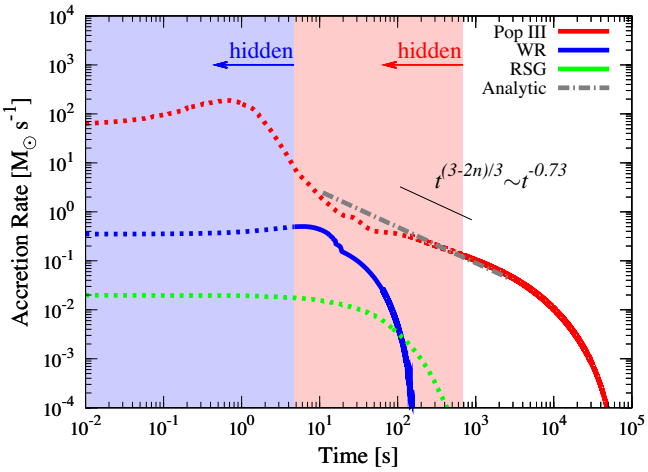

Figure 2. Accretion rates as a function of time. Red, blue, and green lines show Pop III, W-R, and RSG, respectively. Dotted regions represent the jet that propagates inside the star, while the solid regions correspond to the time after the jet breakout for the magnetic jet model. Solid lines give information of observables (e.g., duration and energetics of the GRB). On the other hand, dotted regions show the hidden energy inside the star that goes into the nonrelativistic cocoon component. The gray dot-dashed line represents the analytic model in Equation (13). The black line shows $t^{(3-2n)/3} \sim t^{-0.73}$ as a reference, where $n \sim 2.6$ is a parameter for the density profile (an effective polytropic index of the envelope; see Section 6).

(A color version of this figure is available in the online journal.)

about these mechanisms (e.g., Popham et al. 1999; Di Matteo et al. 2002; Proga et al. 2003; McKinney 2006), we have no concrete consensus for the available energy injection rate from the central engine into the jet. Therefore, we employ two simple models for jet producing mechanisms. We assume that the jet injection luminosity can be written as functions of the accretion rate, $\dot{M}$. The models used in this study are basically written in $\dot{M}$ or $\dot{M}^2$. The accretion-to-jet efficiency is given by the GRB observables with the W-R model in Section 5. More detailed expressions are the following.

1. $L \sim \dot{M}$ model (MHD mechanism): a jet is driven by magnetic fields that are generated by accreting matter.[4] In this case, the jet injection luminosity is given by $L_j = \eta \dot{M} c^2$, where η is the efficiency parameter. In Komissarov & Barkov (2010), $\eta = 0.05/\alpha\beta$, where β is the so-called plasma beta ($\beta = 8\pi P/B^2$, with B being the magnetic field), and we do not know the reliable values for both α and β in the collapsar scenario. Therefore, we parameterize these parameters with η simultaneously.
2. $L \sim \dot{M}^2$ model (neutrino-annihilation mechanism): a jet is driven by the annihilation of neutrinos ($\nu\bar{\nu} \rightarrow e^- e^+$), which are copiously radiated by "hyperaccretion flow" (MacFadyen & Woosley 1999). As for neutrino-annihilation process, the jet injection luminosity is written as $L_j = \zeta \dot{M}^{9/4} M_{\rm BH}^{-3/2}$ (Zalamea & Beloborodov 2010), where ζ is the efficiency parameter including the information about accretion disk, e.g., the spectrum of emitted neutrinos and geometry of disk.

[4] Although the existence of a strong magnetic field in Pop III stars is unclear, there are several studies on the magnetic field amplification (e.g., Sur et al. 2010). Here we assume that the strong magnetic field can be generated at the vicinity of the BH.

4. PENETRATION OF STELLAR ENVELOPE

In this section, we consider the propagation of the jet head in the progenitor star. If a relativistic jet ($\Gamma_j \gg 1$) strikes the stellar matter, two shocks are formed: a forward shock (FS) that accelerates the external material to a Lorentz factor Γ_h, and a reverse shock (RS) that decelerates the head of the jet to Γ_h. Balancing the energy density behind the FS (P_f) with that above the RS (P_r), one can obtain the Lorentz factor of the jet head. As for the ultra-relativistic case ($\Gamma_h \gg 1$), $P_f = \frac{4}{3}\Gamma_h^2 \rho c^2$ and $P_r = \frac{4}{3}(\frac{\Gamma_j}{2\Gamma_h})^2 n_j m_p c^2$, where $n_j = L_{\rm iso}/4\pi r^2 \Gamma_j^2 c$ is the jet proper proton density with $L_{\rm iso}$ being the isotropic luminosity of a jet and m_p is the proton mass, while for the nonrelativistic case ($\Gamma_h \approx 1$), $P_f = \frac{\gamma+1}{2}\rho\beta_h^2 c^2$ and $P_r = \frac{4}{3}\Gamma_j^2 n_j m_p c^2$, where β_h is the velocity of the FS in units of the speed of light, c. These equations lead to the following relations: an ultra-relativistic one, $\Gamma_h \sim L_{\rm iso}^{1/4} r^{-1/2} \rho^{-1/4}$ (Mészáros & Waxman 2001), and a nonrelativistic one, $\beta_h \sim L_{\rm iso}^{1/2} r^{-1} \rho^{-1/2}$ (Waxman & Mészáros 2003). Here we combine these equations empirically as follows:

$$\beta_h \Gamma_h^2 \approx 18 \left(\frac{L_{\rm iso}}{10^{52}\,{\rm erg\,s^{-1}}}\right)^{1/2} \left(\frac{r}{10^{12}\,{\rm cm}}\right)^{-1} \times \left(\frac{\rho}{10^{-7}\,{\rm g\,cm^{-3}}}\right)^{-1/2}. \quad (3)$$

This approximation leads to the same relation as Waxman & Mészáros (2003) for the nonrelativistic case ($\Gamma_h \approx 1$) and agree with Mészáros & Waxman (2001) to within 40% for the ultra-relativistic case ($\beta_h \approx 1$). The crossing time of the FS is also given by

$$t_h \approx \frac{r}{\Gamma_h^2 \beta_h c}. \quad (4)$$

As for the relativistic FS, the crossing time is much shorter than the light crossing time due to its large Lorentz factor (see Mészáros & Rees 2001).

Combining Equations (3) and (4), we obtain the necessary isotropic jet luminosity for the FS to reach the radius r as

$$L_{\rm iso} \approx 3 \times 10^{52} \left(\frac{r}{10^{12}\,{\rm cm}}\right)^4 \left(\frac{\rho}{10^{-7}\,{\rm g\,cm^{-3}}}\right) \left(\frac{t}{1\,{\rm s}}\right)^{-2} {\rm erg\,s^{-1}}. \quad (5)$$

If the jet luminosity decreases slower than t^{-2}, the jet luminosity can achieve this value at the late phase. We can follow the evolution of the FS by equating L_j and Equation (5) including the correction of the jet opening angle, θ_j (i.e., $L_j = L_{\rm iso}\theta_j^2/2$).

We note that the accreting gas from the surrounding to the progenitor star is negligible for the jet breakout since the density of the accreting gas is low, $\rho = \dot{M}/4\pi r^2 v \sim 5 \times 10^{-12}$ g cm^{-3} $(\dot{M}/10^{-2}\ M_\odot\ {\rm yr}^{-1})(r/10^{13}\ {\rm cm})^{-2}$ $(v/10^8\ {\rm cm\ s}^{-1})^{-1}$.

5. GRB AND COCOON

In this section, we divide the energetics of the jet into two components: GRB emitter (relativistic component) and cocoon (nonrelativistic component). When the Lorentz factor of the FS, Γ_h, is smaller than θ_j^{-1}, the shocked material may escape sideways and form the cocoon (Matzner 2003), which avoids the baryon loading problem. With this scenario, the injected energy before the shock breakout goes to the energy of the cocoon and

the energy after breakout goes to the GRB emitter. Therefore, we can calculate the energy budget of the GRB emitter and cocoon after the determination of the jet breakout time, t_b. We define t_b as the maximum time obtained from Equation (5).

First of all, we determine the accretion-to-jet conversion efficiency (depending on the mechanism) using the ordinary GRB progenitor (W-R) to make the total energy of the GRB emitter $E_{\rm tot} = 10^{52}$ erg.[5] In this estimation, we assume that half the opening angle of the jet $\theta_j = 5^\circ$. A successful GRB requires the following two conditions. (1) The jet head reaches the stellar surface. (2) The velocity of the jet head, β_h, should be larger than that of the cocoon, β_c (Matzner 2003; Toma et al. 2007).

As for the $L \sim \dot{M}$ model, the results of the W-R case are $L_j = 1.1 \times 10^{51} (\dot{M}/M_\odot\,{\rm s}^{-1})$ erg s^{-1}, i.e.,

$$\eta = \frac{L_j}{\dot{M}c^2} \approx 6.2 \times 10^{-4}, \tag{6}$$

and $t_{\rm b} = 4.7$ s. For the $L \sim \dot{M}^2$ model, $L_j = 76 \times 10^{51} (\dot{M}/M_\odot\ {\rm s}^{-1})^{9/4} (M_{\rm BH}/M_\odot)^{-3/2}$ erg s^{-1} and $t_{\rm b} = 2.8$ s.[6] We estimate the expected duration of the burst as the period during which 90 percent of the burst's energy is emitted, T_{90}. Both models reproduce the typical burst duration of $\sim$10 s (see Table 1). The energy of the cocoon (injected energy before the shock breakout) is smaller than that of the GRB emitter. The isotropic *kinetic* energy of the GRB emitter is $\sim 10^{54}$ erg.

Next, we apply the above scheme and jet luminosity (e.g., the same η and ζ) to the RSG (progenitor of supernovae without GRBs) and find that the RSG cannot produce GRBs. This is because the jet head is slower than the cocoon. As for W-R with the $L \sim \dot{M}$ model, $\beta_h \sim R_*/(ct_b) \sim 0.3$ and $\beta_c \sim \sqrt{E_c/(Mc^2)} \sim 0.01$, where $E_c \sim 2 \times 10^{51}$ erg is the energy of the cocoon (see Table 1) and $M \sim 10\,M_\odot$ is the stellar mass, hence $\beta_h > \beta_c$. On the other hand, $\beta_h \sim 0.007$ and $\beta_c \sim 0.01$, i.e., $\beta_h \lesssim \beta_c$, for the RSG. Thus, the morphology of the shock wave is almost spherical and the jet cannot break out the stellar surface with a small opening angle. In addition, the FS cannot reach the stellar surface with the $L \sim \dot{M}^2$ model for the RSG. Therefore, our scheme is consistent with observations of the GRB–SN Ibc connection.

Finally, we calculate the evolution of the jet head for the case of the Pop III star (see Table 1). We find that the $L \sim \dot{M}^2$ model does *not* produce GRBs because the FS stalls inside the envelope due to rapidly decreasing jet luminosity (the so-called failed GRB). On the other hand, the $L \sim \dot{M}$ model can supply enough energy for a jet to penetrate the envelope and produce a GRB. Since $\beta_h \sim 0.4$ and $\beta_c \sim 0.08$ in this model, the relativistic jet can penetrate the stellar envelope with a small opening angle and produce a successful GRB. The total energy of the GRB jet (injected energy after breakout) is $\sim$45 times larger than the ordinary GRB and the duration is much longer ($T_{90} \sim 1000$ s). In addition, we estimate the minimum η for a successful breakout, which is $\eta \approx 3.4 \times 10^{-5}$. This is 20 times smaller than that of a normal GRB. In this case $\beta_h \sim 0.03$ and $\beta_c \sim 0.008$. Below this value, the jet head cannot reach the stellar surface.

[5] Note that $E_{\rm tot}$ is not the total energy of gamma rays because there must be a conversion from the kinetic energy of the jet to gamma rays. Though the efficiency of conversion is unclear, it is typically on the order of 0.1. Therefore, we employ $E_{\rm tot} = 10^{52}$ erg that could lead to the true gamma-ray energy of GRB $\sim 10^{51}$ erg.

[6] This luminosity shows a similar value with Equation (22) of Zalamea & Beloborodov (2010) because if $M_{\rm BH} = 3\,M_\odot$, $L_j \approx 16 \times 10^{51}$ erg s^{-1}.

The accretion of the envelope (not core) is very important for Pop III GRBs. Although the envelope is mildly bounded by the gravitational potential (because $\gamma \approx 1.38 \sim 4/3$) and easily escapes when it is heated by the shock, the timescale of the cocoon passing in the envelope ($\sim R_*/(c\beta_c) \sim 3000$ s) is longer than t_b. Therefore, the envelope accretion can last until the jet breakout and our conclusion about the penetrability of the relativistic jet is not changed.

It should be noted that the opening angle of the jet could not be constant during the propagation phase. Due to the additional collimation by the gas pressure, θ_j becomes smaller as the jet propagates (e.g., Zhang et al. 2003; Mizuta et al. 2006, 2010). The smaller θ_j leads to the larger $L_{\rm iso} (= 2L_j/\theta_j^2)$ so that our constant θ_j is a conservative assumption for the jet breakout.

6. ANALYTICAL DEPENDENCES ON PARAMETERS

The hydrogen envelope could be reduced by mass loss, which is one of the most uncertain processes in stellar evolution. Even in zero-metal stars, the synthesized heavy elements could be dredged up to the surface, and might induce the line driven wind. The stellar luminosity could also exceed the Eddington luminosity of the envelope. The stellar pulsation might also blow away the envelope dynamically. So, we analytically estimate the dependence on the envelope mass in the following.

The density profile of the envelope can be written as

$$\rho(r) \approx \rho_1 \left(\frac{R_*}{r} - 1 \right)^n, \tag{7}$$

where n is a constant (Matzner & McKee 1999). This profile is exact if the enclosed mass is constant (i.e., the envelope mass is negligible compared with the core mass) and the equation of state is polytropic, in which case $n = (\gamma - 1)^{-1}$ is a polytropic index. We have $n = 3/2$ for efficiently convective envelopes since the adiabatic index is $\gamma = 5/3$ for the ideal monoatomic gas, and $n = 3$ for radiative envelopes of constant opacity κ since $P \propto \rho^{4/3}$ is derived from the relations, $P_\gamma = (L/L_{\rm Edd})P$, $P \propto \rho T$, and $P_\gamma \propto T^4$, with a constant luminosity-to-mass ratio (L/M) where $L_{\rm Edd} = 4\pi GMc/\kappa > L$ is the Eddington luminosity. We can fit well the Pop III envelope in Figure 1 with $n \approx 2.6$.

Using the profile in Equation (7), we can estimate the envelope mass as

$$M_{\rm env} = \int_{R_c}^{R_*} \rho(r) 4\pi r^2 dr \propto \frac{\rho_1 R_*^3}{3-n} \sim \frac{\rho_c R_c^n R_*^{3-n}}{3-n}, \tag{8}$$

where $\rho_c \equiv \rho(R_c) \approx \rho_1 (R_*/R_c)^n$ is the envelope density just above the core and R_c is the core radius. The core density must be higher than ρ_c to proceed with the nuclear burning. Since the density enhancement is determined by the difference of the ignition temperature, which is not sensitive to other parameters, we assume that the core mass is given by $M_c \propto \rho_c R_c^3$, so that

$$M_{\rm env} \propto \frac{M_c R_c^{n-3} R_*^{3-n}}{3-n}. \tag{9}$$

Then, the stellar radius can be written as a function of the core radius, the core mass, and the envelope mass as follows:

$$R_* \sim 10^{13}\ {\rm cm} \left(\frac{R_c}{10^{10}\ {\rm cm}} \right) \left(\frac{M_c}{400\,M_\odot} \right)^{-2.5} \left(\frac{M_{\rm env}}{500\,M_\odot} \right)^{2.5}, \tag{10}$$

where we use $n = 2.6$ (see the Appendix for n dependences). Therefore, the stellar radius has a strong dependence on the envelope mass. If the envelope mass is smaller than $\sim 50\,M_\odot$, the stellar radius is almost the core radius, $R_c \sim 10^{10}$ cm.

Next, we consider the jet breakout time. Since the accretion time of the core ($r \lesssim 10^{10}$ cm) is $\sim$4 s, the envelope accretion is important for the successful breakout if t_b is longer than this timescale. Using $t_{\rm ff} \sim \sqrt{r^3/GM_r}$, we can evaluate the envelope accretion rate as

$$\dot{M} = \frac{dM_r/dr}{dt_{\rm ff}/dr} \propto \rho_1 M_c^{(3-n)/3} R_*^n t^{(3-2n)/3} \tag{11}$$

with the approximation of $M_r - M_c = \int_{R_c}^{r} \rho(r')4\pi r'^2 dr' \ll M_c \approx 400\,M_\odot$, which is valid for $r \lesssim 10^{12}$ cm (corresponding to $t_{\rm ff} \lesssim 3000$ s). Combining Equations (5), (10), and (11) with $L_j = \eta \dot{M} c^2 = L_{\rm iso}\theta_j^2/2$, the breakout time is given by

$$t_b \sim 700 \left(\frac{\eta}{10^{-3}}\right)^{-0.79} \left(\frac{\theta_j}{5^\circ}\right)^{1.6} \left(\frac{R_c}{10^{10}\,{\rm cm}}\right)^{1.1} \times \left(\frac{M_c}{400\,M_\odot}\right)^{-2.9} \left(\frac{M_{\rm env}}{500\,M_\odot}\right)^{2.8} {\rm s}, \tag{12}$$

where we use $n = 2.6$ (see the Appendix for n dependences) and put $\rho = \rho_1$ and $r = R_*$ in Equation (5). If η is very small ($\lesssim 10^{-5}$) and t_b is longer than the free-fall timescale of the outermost part of the star ($\sim 10^5$ s), the jet cannot penetrate the star. When $\eta \approx 10^{-5}$, $\beta_h \sim R_*/t_b \sim 0.003$ and $\beta_c \sim \sqrt{\eta} \sim 0.003$ so that the shock wave also propagates almost spherically. Similarly, the RSG case in Figure 2 also has too long breakout time since $M_c \sim 4\,M_\odot$ and $M_{\rm env} \sim 11\,M_\odot$.

The jet luminosity after the breakout ($t > t_b$) is given by

$$L_{\rm iso}(t) \sim 5 \times 10^{52} \left(\frac{\eta}{10^{-3}}\right) \left(\frac{\theta_j}{5^\circ}\right)^{-2} \left(\frac{R_c}{10^{10}\,{\rm cm}}\right)^{-0.4} \times \left(\frac{M_c}{400\,M_\odot}\right)^{1.1} \left(\frac{t}{700\,{\rm s}}\right)^{-0.73} {\rm erg\,s^{-1}}, \tag{13}$$

where we use $n = 2.6$ (see the Appendix for n dependences) and $M_c \propto \rho_c R_c^3 \sim \rho_1 (R_*/R_c)^n R_c^3$. Interestingly, the dependence of $L_{\rm iso}(t)$ on the envelope mass is only through the time, t. The relativistic jet emitted after the breakout will produce GRB prompt emission and the jet luminosity decreases with time as $t^{-(2n-3)/3} \sim t^{-0.73}$ in this case. Figure 2 shows this dependence with the gray dot-dashed line, which reproduces well the numerical result (red line) for 10 s $\lesssim t \lesssim$ 3000 s. The parameter dependences just after the breakout (most luminous time, $t = t_b$) are given by Equations (12) and (13) as

$$L_{\rm iso}(t = t_b) \sim 5 \times 10^{52} \left(\frac{\eta}{10^{-3}}\right)^{1.6} \left(\frac{\theta_j}{5^\circ}\right)^{-3.2} \left(\frac{R_c}{10^{10}\,{\rm cm}}\right)^{-1.2} \times \left(\frac{M_c}{400\,M_\odot}\right)^{3.2} \left(\frac{M_{\rm env}}{500\,M_\odot}\right)^{-2.0} {\rm erg\,s^{-1}}, \tag{14}$$

where we use $n = 2.6$ (see also the Appendix).

The active duration of the central engine ($\approx t_b + T_{90}$) is determined by the accretion timescale at $r \sim 10^{12}$ cm, where the density gradient gets larger because $\rho(r) \propto (R_*/r - 1)^n$. The region of $r \lesssim 10^{12}$ cm has $\rho(r) \propto (R_*/r)^n$ so that Equations (12) and (13) are valid, while they are not appropriate for $r \gtrsim 10^{12}$ cm ($M_r \gtrsim M_c + 0.4 M_{\rm env}$) due to the existence of the stellar surface, which leads to the fast decrease of the accretion rate (compare the red and gray lines in Figure 2). So, the duration can be calculated using $t_{\rm ff}$ at $r \sim 0.1 R_*$ with Equation (10) as

$$t_{\rm ff}(r = 0.1R_*) \sim 3000 \left(\frac{R_c}{10^{10}\,{\rm cm}}\right)^{1.5} \left(\frac{M_{\rm c}}{400\,M_\odot}\right)^{-3.8} \times \left(\frac{M_{\rm env}}{500\,M_\odot}\right)^{3.8} \left(\frac{M_c + 0.4M_{\rm env}}{600\,M_\odot}\right)^{-0.5} {\rm s}, \tag{15}$$

where we use $n = 2.6$ (see also the Appendix). This is consistent with the result $t_b + T_{90} \sim 2200$ s in the previous section. At this time, the isotropic luminosity in Equation (13) is given by

$$L_{\rm iso}[t = t_{\rm ff}(r = 0.1R_*)] \sim 2 \times 10^{52} \left(\frac{\eta}{10^{-3}}\right) \left(\frac{\theta_j}{5^\circ}\right)^{-2} \times \left(\frac{R_c}{10^{10}\,{\rm cm}}\right)^{-1.5} \left(\frac{M_c}{400\,M_\odot}\right)^{3.9} \left(\frac{M_{\rm env}}{500\,M_\odot}\right)^{-2.8} \times \left(\frac{M_c + 0.4M_{\rm env}}{600\,M_\odot}\right)^{0.37} {\rm erg\,s^{-1}}, \tag{16}$$

where we use $n = 2.6$ (see also the Appendix). We note that the observables in Equations (14), (15), and (16) carry information of the stellar structure.

7. SUMMARY AND DISCUSSION

We have investigated jet propagation in very massive Pop III stars assuming the accretion-to-jet conversion efficiency of the observed normal GRBs. We find that the jet can potentially break out the stellar surface even if the Pop III star has a massive hydrogen envelope, thanks to the long-lasting accretion of the envelope itself. Even if the accretion-to-jet conversion is less efficient than the ordinary GRBs by a factor of $\sim$20, the jet head can penetrate the stellar envelope and produce GRBs. Although the total energy injected by the jet is as large as $\sim 10^{54}$ erg, more than half is hidden in the stellar interior and the energy injected before the breakout goes into the cocoon component. The large envelope accretion can activate the central engine so that the duration of a Pop III GRB is very long if the hydrogen envelope exists. As a result, the luminosity of a Pop III GRB is modest, being comparable to that of ordinary GRBs.

Considering the Pop III GRB at redshift z, the duration in Equation (15) is

$$T_{\rm GRB} = T_{90}(1+z) \approx 30{,}000\,{\rm s} \left(\frac{1+z}{20}\right), \tag{17}$$

which is much longer than the canonical duration of GRBs, $\sim$20 s. The total isotropic-equivalent energy of the Pop III GRB is

$$E_{\gamma,{\rm iso}} = \varepsilon_\gamma E_{\rm iso} \approx 1.2 \times 10^{55} \left(\frac{\varepsilon_\gamma}{0.1}\right) {\rm erg}, \tag{18}$$

where ε_γ is the conversion efficiency from the jet kinetic energy to gamma rays (see Table 1). It should be noted that this value is comparable to the largest $E_{\gamma,{\rm iso}}$ ever observed, $\approx 9 \times 10^{54}$ erg for GRB 080916C (Abdo et al. 2009). This value is smaller than the estimate of Komissarov & Barkov (2010) and Mészáros & Rees (2010), because we consider the hidden (cocoon) component.

Table 1
Model Summary

Model (Reference)	Final Mass ($M_\odot$)	Radius (10^{11} cm)	Mechanism	t_b (s)	Energy of GRB Emitter (10^{52} erg)	Energy of Cocoon (10^{52} erg)	T_{90} (s)	$E_{\rm iso}$ (10^{54} erg)
W-R	14	0.4	MHD	4.7	1.0	0.23	49	2.6
(Woosley & Heger 2006)			Neutrino	2.8	1.0	0.42	10	2.6
Pop III	915	90	MHD	690	45	57	1500	120
(Ohkubo et al. 2009)			Neutrino	...	...	...	...	...
RSG	13	600	MHD	(5×10^5)	(0.88)	(0.16)	(8.4×10^6)	
(Woosley et al. 2002)			Neutrino	...	...	...	...	...

Notes. The final masses of W-R and RSG are not the same as the initial masses of the progenitors (15 $M_\odot$ and 16 $M_\odot$) because of mass loss due to the stellar wind, while Pop III stars do not undergo mass loss and so their final mass is 915 $M_\odot$. t_b is the time of shock breakout from our calculations (see Section 5). The energy of the GRB emitter is the kinetic energy of the relativistic jet after the breakout. The energy of the cocoon is the injected energy before the breakout. $E_{\rm iso}$ is the isotropic energy of GRB emitter, corrected by half of the opening angle of the jet, $\theta_j = 5^\circ$. The parenthetic values for RSG are just for references because the cocoon velocity is larger than the GRB emitter so that the GRB is not generated.

Since the large isotropic energy is stretched over a long duration, the expected flux just after the breakout is not so bright,

$$F = \frac{\varepsilon_\gamma L_{\rm iso}}{4\pi r_L^2} \sim 10^{-9}\ {\rm erg\ cm^{-2}\ s^{-1}}, \quad (19)$$

where r_L is the luminosity distance, which is smaller than the *Swift* Burst Array Telescope (BAT) sensitivity, $\sim 10^{-8}$ erg cm^{-2} s^{-1}. However, there must be a large variety of luminosity as in ordinary GRBs so that more luminous but rare events might be observable by BAT. Although the cocoon component has large energy, the velocity is so low that it is also difficult to observe. If the cocoon component interacts with the dense wind or ambient medium, it might be observable. This is an interesting future work.

The above discussions strongly depend on the envelope mass because the stellar radius is highly sensitive to the envelope mass. We derive analytical dependences on the model parameters in Section 6, which are applicable to a wide variety of progenitor models. According to the analytical estimates, the smaller envelope leads to the shorter duration and the larger observable luminosity. If $M_{\rm env} \lesssim 50\,M_\odot$, $R_* \sim R_c \sim 10^{10}$ cm (see Equation (10)), $t_b \sim 2$ s (obtained using numerical model as in Section 5), and $T_{90} \sim t_{\rm ff} \sim 4(M/400\,M_\odot)^{-1/2} \times (R_c/10^{10}\ {\rm cm})^{3/2}$ s, both t_b and T_{90} might be extended by a factor of α^{-1} due to the rotation. This is much shorter than the GRBs from Pop III stars with massive envelopes. The mass accreting after the breakout is $\sim 200\,M_\odot$, so that $E_{\gamma,{\rm iso}} \sim 3 \times 10^{54}(\varepsilon_\gamma/0.1)$ erg can be emitted by gamma rays after breakout. The luminosity just after the breakout is $L_{\rm iso} \sim 10^{54}$ erg s^{-1}, i.e., $F \sim 10^{-7}$ erg cm^{-2} s^{-1}, which is much brighter than the case with the massive envelope and observable with the *Swift* BAT, while the duration is very short (~ 2 s at the source frame).

Matter entrainment from the envelope is also crucial for fireball dynamics and the GRB spectra (e.g., Ioka 2010). Since the envelope of the Pop III star is different from that of present-day stars, the GRB appearance is also likely distinct from the observed ones. This is also an interesting future work.

Since we do not have any conclusive central engine scenario, we employ two popular mechanisms in this paper, that is, the magnetic model ($L \sim \dot{M}$) and neutrino-annihilation model ($L \sim \dot{M}^2$). The difference between these models is the dependence of the mass accretion rate. We find that the neutrino-annihilation model cannot penetrate the Pop III stellar envelope, so that no GRB occurs, which is consistent with Fryer et al. (2001), Komissarov & Barkov (2010), and Mészáros & Rees (2010).

We thank A. Heger and T. Ohkubo for providing the progenitor models and P. Mészáros and K. Omukai for valuable discussions. This study was supported in part by the Japan Society for Promotion of Science (JSPS) Research Fellowships (Y.S.) and by the Grant-in-Aid from the Ministry of Education, Culture, Sports, Science and Technology (MEXT) of Japan (Nos. 19047004, 21684014, and 22244019).

APPENDIX

DEPENDENCE ON THE DENSITY INDEX n

Here we explicitly show the dependences on n in Equations (10), (12), (13), (14), (15), and (16) as follows:

$$R_* \propto R_c M_c^{-\frac{1}{3-n}} [(3-n)M_{\rm env}]^{\frac{1}{3-n}}, \quad (A1)$$

$$t_b \propto \eta^{-\frac{3}{9-2n}} \theta_j^{\frac{6}{9-2n}} R_c^{\frac{3(4-n)}{9-2n}} M_c^{-\frac{n^2-9n+21}{(3-n)(9-2n)}} [(3-n)M_{\rm env}]^{\frac{3(4-n)}{(3-n)(9-2n)}}, \quad (A2)$$

$$L_{\rm iso}(t) \propto \eta \theta_j^{-2} R_c^{-(3-n)} M_c^{\frac{6-n}{3}} t^{-\frac{2n-3}{3}}, \quad (A3)$$

$$L_{\rm iso}(t=t_b) \propto \eta^{\frac{6}{9-2n}} \theta_j^{-\frac{12}{9-2n}} R_c^{-\frac{15-4n}{9-2n}} \times M_c^{\frac{2n^2-16n+33}{(3-n)(9-2n)}} [(3-n)M_{\rm env}]^{-\frac{(4-n)(2n-3)}{(3-n)(9-2n)}}, \quad (A4)$$

$$t_{\rm ff}(r=0.1R_*) \propto R_c^{\frac{3}{2}} M_c^{-\frac{3}{2(3-n)}} [(3-n)M_{\rm env}]^{\frac{3}{2(3-n)}} \times (M_c + 0.4M_{\rm env})^{-\frac{1}{2}}, \quad (A5)$$

$$L_{\rm iso}[t=t_{\rm ff}(r=0.1R_*)] \propto \eta \theta_j^{-2} R_c^{-\frac{3}{2}} M_c^{\frac{2n^2-12n+27}{6(3-n)}} \times [(3-n)M_{\rm env}]^{\frac{3-2n}{2(3-n)}} (M_c + 0.4M_{\rm env})^{\frac{2n-3}{6}}. \quad (A6)$$

We note that the total energy is proportional to

$$t_{\rm ff}(r=0.1R_*) L_{\rm iso}[t=t_{\rm ff}(r=0.1R_*)] \propto \eta \theta_j^{-2} M_c^{\frac{3-n}{3}} \times [(3-n)M_{\rm env}](M_c + 0.4M_{\rm env})^{-\frac{3-n}{3}}, \quad (A7)$$

if $n < 3$ (i.e., $L_{\rm iso}(t)$ is shallower than t^{-1}).

REFERENCES

Abdo, A. A., et al. 2009, Science, 323, 1688
Abdo, A. A., et al. 2010, ApJ, 723, 1082
Abel, T., Bryan, G. L., & Norman, M. L. 2002, Science, 295, 93
Barkana, R., & Loeb, A. 2001, Phys. Rep., 349, 125
Begelman, M. C., & Cioffi, D. F. 1989, ApJ, 345, L21
Blandford, R. D., & Znajek, R. L. 1977, MNRAS, 179, 433
Bromm, V., Coppi, P. S., & Larson, R. B. 2002, ApJ, 564, 23
Bromm, V., & Larson, R. B. 2004, ARA&A, 42, 79
Bromm, V., & Loeb, A. 2006, ApJ, 642, 382
Chandra, P., et al. 2010, ApJ, 712, L31
Ciardi, B., & Ferrara, A. 2005, Space Sci. Rev., 116, 625
Ciardi, B., & Loeb, A. 2000, ApJ, 540, 687
Clark, P. C., Glover, S. C. O., Klessen, R. S., & Bromm, V. 2010, arXiv:1006.1508
Di Matteo, T., Perna, R., & Narayan, R. 2002, ApJ, 579, 706
Fryer, C. L., Woosley, S. E., & Heger, A. 2001, ApJ, 550, 372
Gou, L. J., Mészáros, P., Abel, T., & Zhang, B. 2004, ApJ, 604, 508
Greiner, J., et al. 2009, ApJ, 693, 1610
Heger, A., Fryer, C. L., Woosley, S. E., Langer, N., & Hartmann, D. H. 2003, ApJ, 591, 288
Inoue, S. 2004, MNRAS, 348, 999
Inoue, S., Omukai, K., & Ciardi, B. 2007, MNRAS, 380, 1715
Inoue, S., Salvaterra, R., Choudhury, T. R., Ferrara, A., Ciardi, B., & Schneider, R. 2010, MNRAS, 404, 1938
Ioka, K. 2003, ApJ, 598, L79
Ioka, K. 2010, Prog. Theor. Phys., 124, 667
Ioka, K., & Mészáros, P. 2005, ApJ, 619, 684
Kawai, N., et al. 2006, Nature, 440, 184
Kistler, M. D., Yüksel, H., Beacom, J. F., Hopkins, A. M., & Wyithe, J. S. B. 2009, ApJ, 705, L104
Komissarov, S. S., & Barkov, M. V. 2010, MNRAS, 402, L25
Kudritzki, R. P. 2002, ApJ, 577, 389
Kumar, P., Narayan, R., & Johnson, J. L. 2008, Science, 321, 376
Lamb, D. Q., & Reichart, D. E. 2000, ApJ, 536, 1
MacFadyen, A. I., & Woosley, S. E. 1999, ApJ, 524, 262
Madau, P., & Rees, M. J. 2001, ApJ, 551, L27
Matzner, C. D. 2003, MNRAS, 345, 575
Matzner, C. D., & McKee, C. F. 1999, ApJ, 510, 379
McKinney, J. C. 2006, MNRAS, 368, 1561
Mészáros, P., & Rees, M. J. 2001, ApJ, 556, L37
Mészáros, P., & Rees, M. J. 2010, ApJ, 715, 967
Mészáros, P., & Waxman, E. 2001, Phys. Rev. Lett., 87, 171102
Miralda-Escude, J. 1998, ApJ, 501, 15
Mizuta, A., Nagataki, S., & Aoi, J. 2010, arXiv:1006.2440
Mizuta, A., Yamasaki, T., Nagataki, S., & Mineshige, S. 2006, ApJ, 651, 960
Naoz, S., & Bromberg, O. 2007, MNRAS, 380, 757
Oh, S. P. 2001, ApJ, 553, 25
Ohkubo, T., Nomoto, K., Umeda, H., Yoshida, N., & Tsuruta, S. 2009, ApJ, 706, 1184
Omukai, K., & Palla, F. 2003, ApJ, 589, 677
Perna, R., & MacFadyen, A. 2010, ApJ, 710, L103
Popham, R., Woosley, S. E., & Fryer, C. 1999, ApJ, 518, 356
Proga, D., MacFadyen, A. I., Armitage, P. J., & Begelman, M. C. 2003, ApJ, 599, L5
Salvaterra, R., et al. 2009, Nature, 461, 1258
Schaefer, B. E. 2007, ApJ, 660, 16
Sur, S., Schleicher, D. R. G., Banerjee, R., Federrath, C., & Klessen, R. S. 2010, ApJ, 721, L134
Suwa, Y., Takiwaki, T., Kotake, K., & Sato, K. 2007a, ApJ, 665, L43
Suwa, Y., Takiwaki, T., Kotake, K., & Sato, K. 2007b, PASJ, 59, 771
Suwa, Y., Takiwaki, T., Kotake, K., & Sato, K. 2009, ApJ, 690, 913
Tanvir, N. R., et al. 2009, Nature, 461, 1254
Toma, K., Ioka, K., Sakamoto, T., & Nakamura, T. 2007, ApJ, 659, 1420
Toma, K., Sakamoto, T., & Meszaros, P. 2010, arXiv:1008.1269
Totani, T. 1997, ApJ, 486, L71
Totani, T., Kawai, N., Kosugi, G., Aoki, K., Yamada, T., Iye, M., Ohta, K., & Hattori, T. 2006, PASJ, 58, 485
Turk, M. J., Abel, T., & O'Shea, B. 2009, Science, 325, 601
Waxman, E., & Mészáros, P. 2003, ApJ, 584, 390
Woosley, S. E., & Bloom, J. S. 2006, ARA&A, 44, 507
Woosley, S. E., & Heger, A. 2006, ApJ, 637, 914
Woosley, S. E., Heger, A., & Weaver, T. A. 2002, Rev. Mod. Phys., 74, 1015
Yonetoku, D., Murakami, T., Nakamura, T., Yamazaki, R., Inoue, A. K., & Ioka, K. 2004, ApJ, 609, 935
Yoon, S.-C., & Langer, N. 2005, A&A, 443, 643
Yoshida, N., Omukai, K., & Hernquist, L. 2008, Science, 321, 669
Zalamea, I., & Beloborodov, A. M. 2010, arXiv:1003.0710
Zhang, W., Woosley, S. E., & MacFadyen, A. I. 2003, ApJ, 586, 356